

# Spatio-Temporal Variability of Shallow Groundwater Quality in a Hilly Red-Soil Agricultural Catchment in Subtropical Central China

Qiao Luo<sup>1,2,3</sup>, Yong Li<sup>1,2\*</sup>, Yuyuan Li<sup>1,2</sup>, Xinliang Liu<sup>1,2,3</sup>, Runlin Xiao<sup>1,2</sup>, Jinshui Wu<sup>1,2</sup>

<sup>1</sup>Key Laboratory of Agro-Ecological Processes in Subtropical Region, Institute of Subtropical Agriculture, Chinese Academy of Sciences, Changsha, China

<sup>2</sup>Changsha Research Station for Agricultural & Environmental Monitoring, Changsha, China

<sup>3</sup>The University of Chinese Academy of Sciences, Beijing, China

Email: \*[yli@isa.ac.cn](mailto:yli@isa.ac.cn)

Received 22 December 2014; accepted 5 January 2015; published 14 January 2015

Copyright © 2015 by authors and Scientific Research Publishing Inc.

This work is licensed under the Creative Commons Attribution International License (CC BY).

<http://creativecommons.org/licenses/by/4.0/>



Open Access

---

## Abstract

Groundwater quality varies not only in space but also in time. In order to analyze the spatio-temporal variety of ground water quality, the concentration of ammonium nitrogen ( $\text{NH}_4\text{N}$ ), nitrate nitrogen ( $\text{NO}_3\text{N}$ ), total nitrogen (TN) and total phosphorus (TP) in very shallow groundwater were investigated in a red-soil catchment in subtropical central China, based on a three-dimensional kriging method. The spatio-temporal analysis demonstrated that  $\text{NH}_4\text{N}$ ,  $\text{NO}_3\text{N}$  and TP presented strong spatio-temporal autocorrelation (with a nugget-to-sill ratio of <25%) and that TN presented a moderate spatio-temporal autocorrelation (with a nugget-to-sill ratio between 25% and 75%). According to the Chinese Groundwater Quality Standards, the ratio of areas contaminated by  $\text{NH}_4\text{N}$ ,  $\text{NO}_3\text{N}$ , TN and TP to the whole catchment was 20.05%, 1.46%, 5.07%, 5.98%, respectively. The 3D delineation of continuously dynamic variation of contaminated area indicated that the catchment's very shallow groundwater had a moderate contamination by  $\text{NH}_4\text{N}$ , slight by TN and TP, and almost non by  $\text{NO}_3\text{N}$ . Although the contaminated area was very small, only occurring in small dispersed patches, a close attention should be paid to the shallow groundwater quality because local farmers obtain their domestic drinking water directly from this shallow groundwater without any treatment prior to consuming and the potential health hazard is considerable. The findings from this study highlight the importance of surveillance of the contaminated area over time for decision making to protect public health and maintain sustainable development of

---

\*Corresponding author.

the catchment.

## Keywords

Drinking Water, Nitrogen, Phosphorus, 3D Spatio-Temporal Geostatistics

## 1. Introduction

In rural areas of China, the shallow groundwater is the source of drinking water for local farmers. The quality of the groundwater may be affected by the use of agrochemicals [1], especially the nitrogen (N) and phosphorus (P) fertilizers. High N and P concentrations in groundwater could pose risks to environmental quality and have potential hazards to human health including methemoglobinemia, gastric cancer, and non-Hodgkin's lymphoma [2]. The threshold of the nitrate-N ( $\text{NO}_3\text{N}$ ) concentration in drinking water for safe drinking was recommended as 11 mg/L by the World Health Organization and as 10 mg/L by the US Environmental Protection Agency. In the UK, the groundwater P concentration is frequently monitored against the EU drinking water standard of 2.2 mg/L [3]. According to the Chinese Groundwater Quality Standards, thresholds of 1.0 mg/L for  $\text{NH}_4\text{N}$ , 10 mg/L for  $\text{NO}_3\text{N}$  and 0.2 mg/L for TP in potable water were set, respectively. Assessing the groundwater quality and identifying contaminated areas play a vital role in protecting public health. However, water quality varies over both space and time [4]. Spatially, numerous studies have documented the distribution of  $\text{NO}_3\text{-N}$  in groundwater and relationship between  $\text{NO}_3\text{-N}$  in groundwater and agricultural activities [5] [6], land use [7], hydraulic conditions [8], topographic characteristics [9]. Temporally, historical records showed that  $\text{NO}_3\text{-N}$  increased from about 2 mg/L in the early 1940s to about 15 mg/L in 2002 in the US [10]. According to [11], the concentrations of N and P during the rainy season were higher than in other months in the Taihu Lake region of China.  $\text{NO}_3\text{-N}$  has already been reported as high as 67 mg/L in northern china [12]. Relatively high concentrations of P have been reported for some groundwater bodies [3] [13]. There were also studies in both spatial and temporal variations of nutrients ( $\text{NO}_3^-$ ,  $\text{PO}_4^{3-}$ ,  $\text{NH}_4^+$ ) in groundwater quality [4]. However, these studies separated space from time, only focusing on geostatistical analysis on spatial characteristics or conventional analysis on temporal trends solely. N and P in the groundwater often follow complex hydrological pathways [14] [15] and have impacts over the catchment scale. Moreover, the concentration of N and P are also affected by the weather condition such as precipitation and agricultural activities such as fertilizing which occurred chronologically, and the current status of N and P have impacts on their succedent status. Therefore, it is essential to integrate spatial characteristics and temporal trends of groundwater quality with respect to both N and P at catchment scale. In the last decades, several efforts have been made for the spatio-temporal modeling [16]. Reference [17] derived a spectral approach that allowed one to obtain many classes of non-separable, spatio-temporal stationary covariance functions, and [18] worked a natural generalization by using completely monotone functions and functions whose first derivative was completely monotone [16]. References [19] and [20] introduced a product-sum model. A Bayesian maximum entropy (BME) method was used for the space/time estimation of Petrachloroethylene in New Jersey [21]. Reference [22] applied three fully spatio-temporal methods to interpolate PM10 measurements in Europe: a metric model (3D kriging), a separable covariance function and a product-sum covariance function, and found that the 3D kriging approach performed best based on the statistical analysis. The 3D kriging assumes time to be a third orthogonal dimension with identical correlation structure for spatial, temporal and spatio-temporal distances. Thus, the space-time variable of interest is treated as a sum of independent stationary spatial, temporal, and spatio-temporal components, which leads to a sum-metric space-time semivariogram model.

The Jinjing River, which is located in southern subtropical China, is a headwater tributary of the middle reach of the Yangtze River. The Jinjing catchment, which is a hilly red-soil agricultural catchment, is at risk of pollution due to excessive nutrient inputs from point and nonpoint sources. Therefore, it is important to investigate the variability of groundwater quality to identify when, where and how severe the groundwater is contaminated in this catchment. In this study, the 3D spatio-temporal analysis was performed to evaluate the spatio-temporal variability of very shallow groundwater quality throughout the Jinjing catchment.

## 2. Materials and Methods

### 2.1. Study Area

This study was carried out in the Jinjing catchment in Changsha County, Hunan province (**Figure 1**) which covers an area of 135 km<sup>2</sup>. The climate is characterized as subtropical moist monsoon. The annual precipitation was 1330 mm (1955-2010), 66.5% of which fell during the warm and rainy season from May to August. The annual mean air temperature was 17.5°C (1955-2010). The topography of the area is hilly with elevation ranging from 52 to 494 m above sea level. The two dominant soil types are Ultisols (USDA soil classification), or Kastanozems (FAO/UNESCO soil classification) or red soils (Chinese soil classification) (57%), which was mainly derived from slate shale and granite, and Inceptisols (USDA soil classification) or Anthrosols (FAO/UNESCO soil classification) or paddy soils (Chinese soil classification) (42%), which was derived from alluvial deposit of rivers. The average soil pH is 4.5 [23]. The average groundwater depth below the soil surface is 0.5 m to 5.0 m across the entire catchment. Woodland (65%) and paddy fields (27%) are the primary land-use types in the region. The study area has been dominated by a double rice cropping management.

### 2.2. Groundwater Sampling

A total of 199 Polyvinyl chloride (PVC) pipes with inside diameters of 5 cm were installed throughout the catchment in April 2010 for groundwater sampling. These PVC pipes reached various depths (100 to 130 cm) depending on soil character. The bottom of the pipes was designed for clay soil to allow the penetration of groundwater into the pipe. A hand vacuum pump was used to sample the accumulated shallow groundwater in the pipes. Each pipe was sampled monthly in 2011. The locations of the pipes were determined by a hand-held Global Positioning System (GPS) receiver and are shown in **Figure 1**. All the water samples were collected in pre-cleaned polythene bottles (500 ml), stored in the insulation box and transported to the laboratory in two hours. Samples were then stored in a freezer at -20°C and subsequently the analyses for NH<sub>4</sub>N, NO<sub>3</sub>N, TN and TP were carried out within two weeks using a FOSS FIAstar 5000 Flow Injection Analyzer. Once the samples were taken out of the freezer, their chemical analyses were finished in 12 hours.

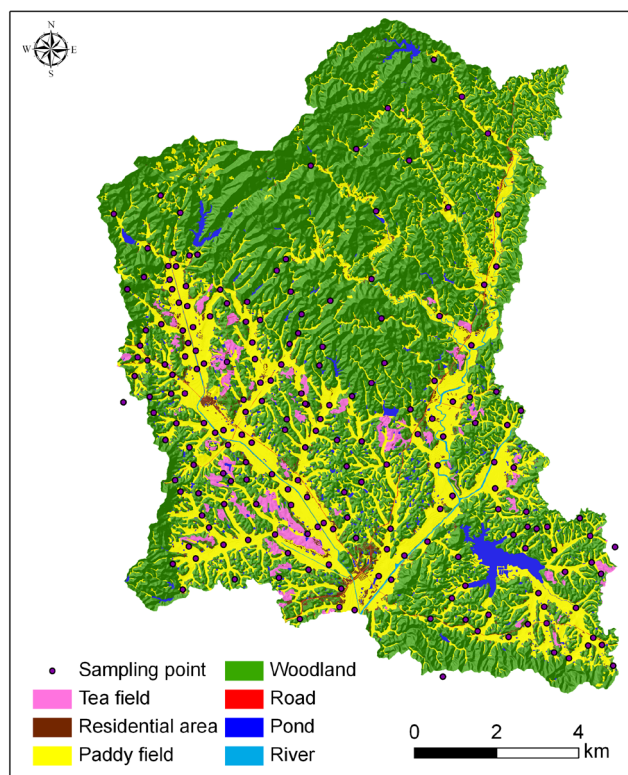


**Figure 1.** Sampling points and land use type in Jinjing catchment.

### 2.3. Data Preprocessing

Summary statistics of the data are shown in **Table 1**. The mean concentration of NH<sub>4</sub>N, NO<sub>3</sub>N, TN and TP was 1.192, 1.112, 2.836 and 0.071 mg/L, respectively. The skewnesses revealed asymmetry and the kurtosises showed a stretching of the distribution of the data. The logit-transformation normalized the data and reduced this asymmetry.

### 2.4. Three Dimensional Kriging

For analyzing the spatio-temporal variability of ground water quality, we considered time as the third orthogonal dimension leading to a natural spatio-temporal 3-dimensional kriging (3D kriging) extension of spatial 2-dimensional kriging (2D kriging). Considering that the unit of distance in time was not the same as the unit of distance in space, one month was assumed to correspond to a distance of 500 meters [22]. Such an assumption enabled the researchers to generate a single spatio-temporal semivariogram and predict any point in the space-time cube. Under the intrinsic stationarity assumption, the spatio-temporal logit-transformed semivariograms in three dimensions were then calculated as the following:

$$\lambda(h_{st}) = [2N(h_{st})]^{-1} \sum_{i=1}^{N(h_{st})} [Z(x_i) - Z(x_i + h_{st})]^2 \quad (1)$$

where  $h_{st}$  is the spatio-temporal lags,  $N(h_{st})$  is the number of pairs of observations with the same distance  $h_{st}$ ,  $Z(x_i)$  and  $Z(x_i + h_{st})$  is the spatio-temporal observations at point  $x_i$  and  $x_i + h_{st}$ , respectively. To predict the value of  $Z$  at any unobserved points, the 3D kriging yields the best unbiased linear predictor of  $Z(x_0)$  as:

$$Z^*(x_0) = \sum_{i=1}^n \lambda_i Z(x_i) \quad (2)$$

with

$$\sum_{i=1}^n \lambda_i = 1 \quad (3)$$

where  $Z^*(x_0)$  is the estimated value of  $Z$  at the unobserved point  $x_0$ , and  $\lambda_i$  is the  $n$  weights assigned to the observation points  $Z(x_i)$  located in the neighborhood with the sum of  $\lambda_i$  equals to 1.

Five parameters, including three angles (ang1, ang2, and ang3) and two ratios (k1 and k2), should be given in 3D kriging when geometric anisotropy was considered. ang1 refers to the principal direction of continuity (measured in degrees, clockwise from  $Y$ , in direction of  $X$ ), ang2 is the dip angle for the principal direction of continuity (measured in positive degrees up from horizontal), and ang3 is the third rotation angle which rotates

**Table 1.** Statistical summary of original and logit transformed NH<sub>4</sub>N, NO<sub>3</sub>N, TN and TP.

	Original				Logit Transformed			
	NH <sub>4</sub> N	NO <sub>3</sub> N	TN	TP	Logit-NH <sub>4</sub> N	Logit-NO <sub>3</sub> N	Logit-TN	Logit-TP
Number of Points	1850	1850	1849	1849	1850	1850	1849	1849
Minimum	0.000	0.000	0.000	0.000	-11.170	-10.650	-11.510	-9.306
1 <sup>st</sup> Qu.	0.026	0.174	0.710	0.016	-7.874	-5.476	-4.939	-6.471
Median	0.068	0.483	1.385	0.029	-6.935	-4.453	-4.265	-5.902
Mean	1.192	1.112	2.836	0.071	-6.440	-4.789	-4.190	-5.841
3 <sup>rd</sup> Qu.	0.619	1.109	2.803	0.052	-4.732	-3.607	-3.546	-5.331
Maximum	70.877	40.170	98.200	9.513	6.357	3.089	4.002	1.856
Kurtosis	121.667	78.276	93.815	693.037	3.328	4.855	6.284	6.064
Skewness	9.399	7.337	7.727	22.990	0.299	-1.048	0.593	0.259

the two minor directions around the principal direction defined by  $\text{ang1}$  and  $\text{ang2}$ . Anisotropy  $k1$  and  $k2$  are the ratios between the major range and each of the two minor ranges. By introducing a coordinate transformation matrix, anisotropy can be reduced to isotropy [24].

These approaches were implemented in R [25] and heavily rely on the R package *gstat*.

## 2.5. Evaluation Standards of Groundwater Quality

There were three evaluation standards in terms of groundwater or drinking water quality in China, which were environmental quality standards for surface water, quality standards for ground water and drinking water. Quality standards for ground water and drinking water were not adopted because there were no criteria for TN and TP in both of them. According to environmental quality standards for surface water for criterion III which is legislated for drinking water, the thresholds of the safe level for  $\text{NH}_4\text{-N}$ ,  $\text{NO}_3\text{-N}$ , TN and TP are 1.0, 10, 1.0 and 0.2 mg/L, respectively. However, it is surprising that the threshold of the safe level for TN (1.0 mg/L) was much lower than that of  $\text{NO}_3\text{-N}$  (10 mg/L). The threshold of the safe level for  $\text{NO}_3\text{-N}$  in drinking water is recommended as 10 mg/L by the USA, which is consistent with that recommended by GB 3838-2002. Therefore, the safe level for TN was set to 10 mg/L in this study. Therefore, the thresholds of the safe level for  $\text{NH}_4\text{-N}$ ,  $\text{NO}_3\text{-N}$ , TN and TP are 1.0, 10, 10 and 0.2 mg/L, respectively.

## 3. Results and Discussion

### 3.1. Spatio-Temporal Statistics

The logit-transformed spatio-temporal semivariograms of the four groundwater quality variables are shown in **Figure 2**. The range of  $\text{NH}_4\text{N}$ ,  $\text{NO}_3\text{N}$ , TN and TP was 828 m, 836 m, 1079 m and 811 m, respectively (**Figure 2**). The computed model parameters are presented in **Table 2**. The fitted semivariogram models for the four variables are all Stein's parameterized Matern (ste). The spatio-temporal semivariogram may be affected by intrinsic and/or extrinsic factors and can be classified into three categories according to a nugget-to-sill ratio (%), with a ratio of <25% indicating a strong spatio-temporal dependence, a ratio of 25% - 75% indicating a moderate spatio-temporal dependence and a ratio of >75% indicating a weak spatio-temporal dependence [26]. In this study, it is noteworthy that all the ratios of nugget-to-sill for  $\text{NH}_4\text{N}$ ,  $\text{NO}_3\text{N}$ , and TP equal to zero as well, which showed a strong spatio-temporal dependence which might be completely attributed to intrinsic factors (e.g., physical, chemical, and biological characteristics of the landscape, and hydraulic and geographic conditions). In addition, the ratio of nugget-to-sill for TN is 35%, showing a moderate spatio-temporal dependence, which might be both determined by extrinsic factors (e.g., fertilizer application and animal wastes) and intrinsic factors. Anisotropy parameters are also shown in **Table 2**. It is noteworthy that the distribution of TP was isotropic.

Leave-One-Out cross-validation analysis was performed to evaluate the accuracy of the interpolation of the 3D kriging. The mean prediction error (ME) and the root mean squared error (RMSE) were then used to evaluate the performance of the interpolation, as well as the correlation coefficient ( $r$ ). Ideally, ME should be close to zero, RMSE should be as small as possible, and  $r$  should be close to 1. The result of leave-one-out cross validation analysis was shown in **Table 2**. It was found that the ME was close to 0 (between -0.019 and -0.00005), the RMSE ranged from 0.867 to 1.843 and  $r$  ranged from 0.38 to 0.64, indicating an accuracy of predictions.

### 3.2. Spatio-Temporal Distributions

**$\text{NH}_4\text{N}$ .** As shown in **Figure 3**, the concentration of  $\text{NH}_4\text{N}$  was high (up to 70 mg/L) which occurred in April, exceeding the safety threshold of 1.0 mg/L by 70 times. 20.05% of the data collected from January to December exceeded the safety threshold. The concentration of  $\text{NH}_4\text{N}$  is less than 0.15 mg/L for most area of the catchment. It is noteworthy that there is always a high ammonium concentration center in the northeast of the catchment, especially in May, June and July, which is shown as red in **Figure 3**.

**$\text{NO}_3\text{N}$ .** As shown in **Figure 4**, the highest concentration of  $\text{NO}_3\text{N}$  reached 40 mg/L, exceeding the safety threshold of 10 mg/L by 4 times, although only 1.46% of the observations exceeded the safety threshold. The maximum nitrate concentration just occurred in January as a point, standing till April. Most areas of the catchment remain uncontaminated by  $\text{NO}_3\text{N}$  with concentrations between 0.2 and 0.5 mg/L.

**TN.** As shown in **Figure 5**, the highest concentration of TN reached 55 mg/L, exceeding the safety threshold

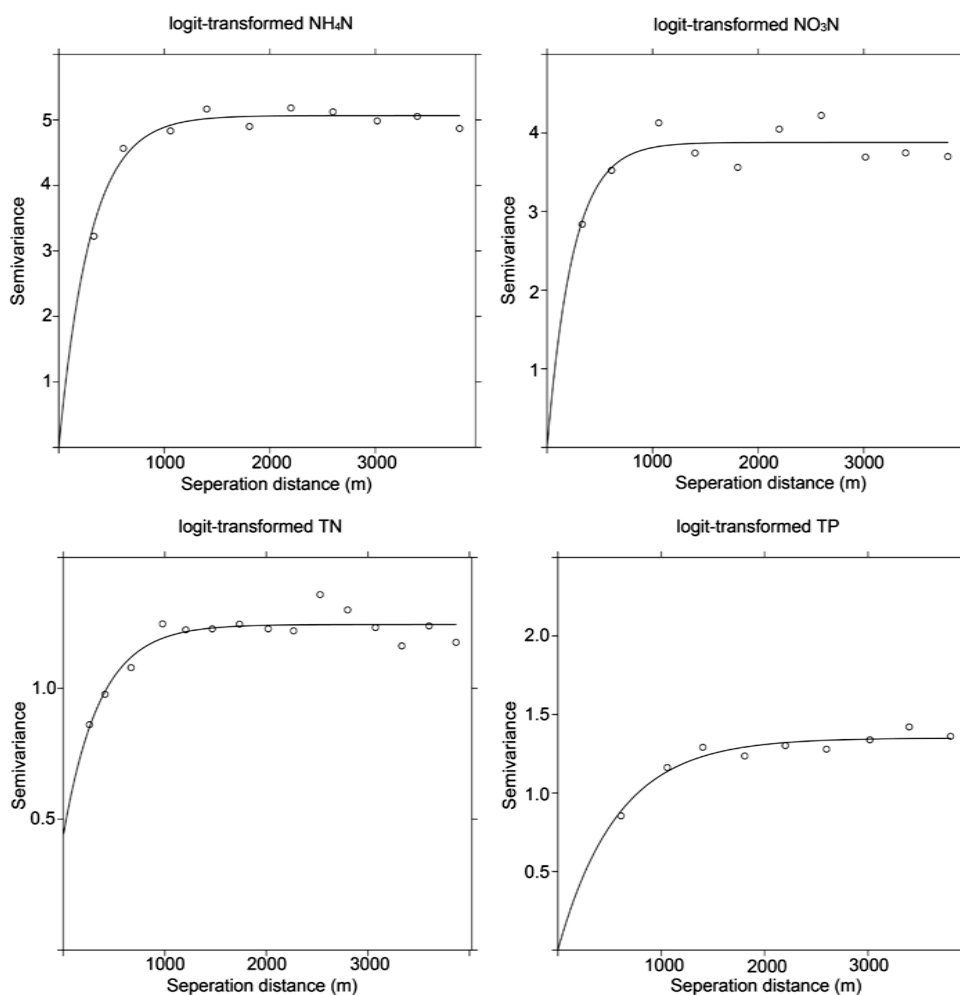


**Figure 2.** Three dimensional semivariance of the logit-transformed ammonium nitrogen ( $\text{NH}_4\text{N}$ ), nitrate nitrogen ( $\text{NO}_3\text{N}$ ), total nitrogen (TN) and total phosphorus (TP) concentrations. Distance corresponds to meters, where a temporal difference of 1 month equals 500 m. The semivariance in X-Y planes, Z plane, and X-Y-Z planes represented spatial, temporal, and spatio-temporal semivariance respectively.

**Table 2.** Model parameters for 3D semivariograms of logit-transformed  $\text{NH}_4\text{N}$ ,  $\text{NO}_3\text{N}$ , TN and TP concentrations.

Variable	Semivariogram model parameter				Anisotropy parameter				Leave-one-out cross validation			
	Range (m)	Model	Nugget	Psill	Ang1 (degree)	Ang2 (degree)	Ang3 (degree)	Ratio1	Ratio2	ME	RMSE	r
$\text{NH}_4\text{N}$	828	ste	0	5.065	90	90	0	0.51	0.49	-0.015	1.843	0.62
$\text{NO}_3\text{N}$	836	ste	0	3.88	95	100	102	0.5	0.415	-0.00005	1.552	0.62
TN	1079	ste	0.437	0.806	84	82	0	0.469	0.509	-0.019	0.867	0.64
TP	811	ste	0	1.35	-	-	-	-	-	0.009	1.071	0.38

of 10 mg/L 5.5 by times, and 5.07% of the observations exceeded the safety threshold. Compared with spatio-temporal variability of  $\text{NH}_4\text{N}$  in Figure 3, the high TN concentration center appeared in May, June and July, which was consistent with that of  $\text{NH}_4\text{N}$  in the northeast of the catchment. While compared with spatio-temporal variability of  $\text{NO}_3\text{N}$  in Figure 4, the high TN concentration center appeared in January, February, March and April was also demonstrated in Figure 5. Except for the high TN concentration centers, most areas of the catchment remain uncontaminated by TN with concentrations between 1.0 and 2.0 mg/L.

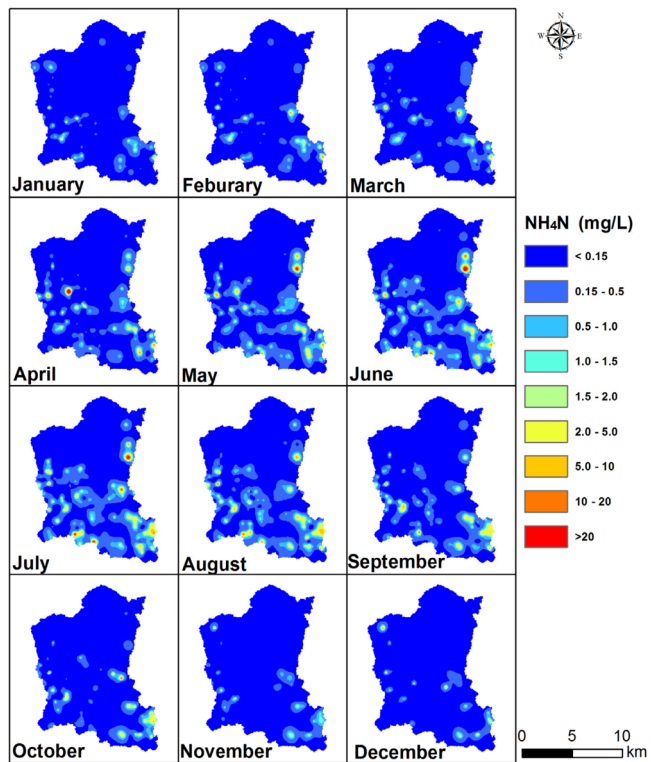


Figure 3. Estimated  $\text{NH}_4\text{N}$  over Jinjing catchment from January to December in 2011 monthly, mg/L.

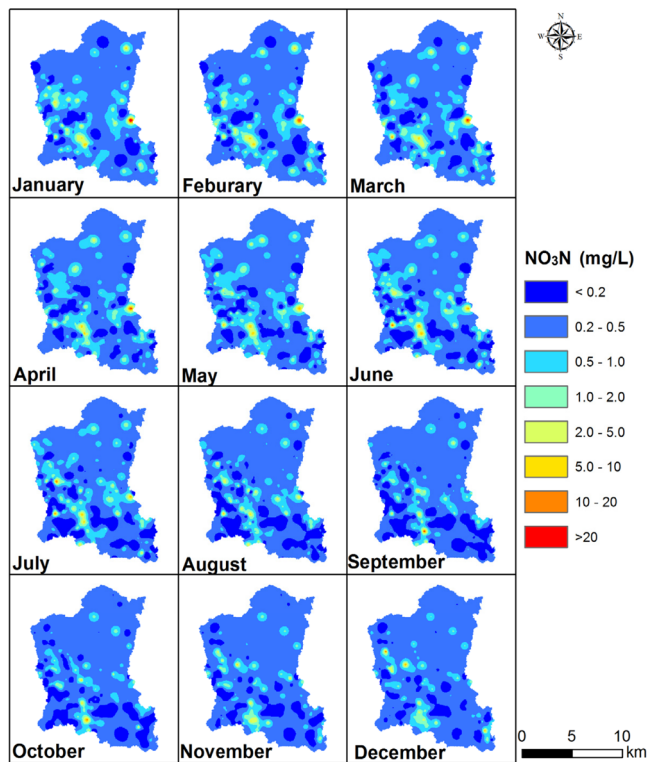
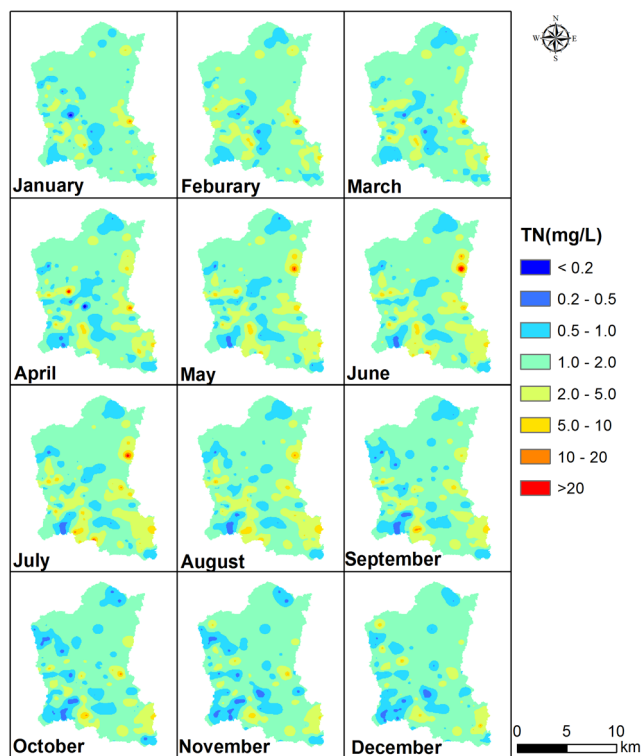


Figure 4. Estimated  $\text{NO}_3\text{N}$  over Jinjing catchment from January to December in 2011 monthly, mg/L.



**Figure 5.** Estimated TN over Jinjing catchment from January to December in 2011 monthly, mg/L.

**TP.** As shown in **Figure 6**, the highest concentration of TP reached 10 mg/L, exceeding the safety threshold of 0.2 mg/L by 50 times, and 5.98% of the observations exceeded the safety threshold. Most of the area in the catchment remains uncontaminated by TP with concentrations between 0.02 and 0.1 mg/L. The high TP concentration centers flashed in the center of the Jinjing catchment in April and in December. In addition, there were two hot-spots in northeast and south of the area in May and June, suggesting the existence of the potential anthropogenic point sources.

**Figure 7** portrays the continuously dynamic variation of contaminated area of  $\text{NH}_4\text{N}$ ,  $\text{NO}_3\text{N}$ , TN and TP. Comparing numbers and volume of spatio-temporal cube in **Figures 7(a)-(d)**, the catchment was more seriously polluted by  $\text{NH}_4\text{-N}$ , moderately polluted by TP and TN, and lowest polluted by  $\text{NO}_3\text{-N}$ . Contamination of  $\text{NH}_4\text{-N}$  mainly occurred in May, June, July and August, which was during the period of rice growth and fertilizer application, indicating that rice agriculture had a negative effect on the shallow groundwater quality. The higher contamination level of  $\text{NH}_4\text{-N}$  than that of  $\text{NO}_3\text{-N}$  might be attributed to the low nitrification rate. For one thing, red soil (Ultisols and Oxisols in US Soil Taxonomy) is the dominant soil type in this catchment with a low pH of 4.5 [23] resulting in a low nitrification potential. For another, the short distance between top soil and shallow groundwater, which was only 100 to 130 cm, restrict the nitrification time, resulting in small rates of nitrification. Further investigation of soil and deep groundwater  $\text{NH}_4\text{N}$  and  $\text{NO}_3\text{N}$  concentration is needed to clarify this problem.

Most of the area in the catchment was not contaminated by TP, due to the fact that phosphorus can be adsorbed by natural sediments and pure minerals in soil, resulting in small rates of phosphorus transport to groundwater [11]. Generally, transport of phosphorus to groundwater is assumed to be not important because of the high potential for mobile phosphorus to be retained in the upper soil horizons by adsorption or metal complex formation [27].

#### 4. Conclusions

This study investigated the potential of 3D kriging approach for spatio-temporal variability of groundwater quality with  $\text{NH}_4\text{N}$ ,  $\text{NO}_3\text{N}$ , TN and TP concentrations which were measured monthly in the Jinjing catchment for the

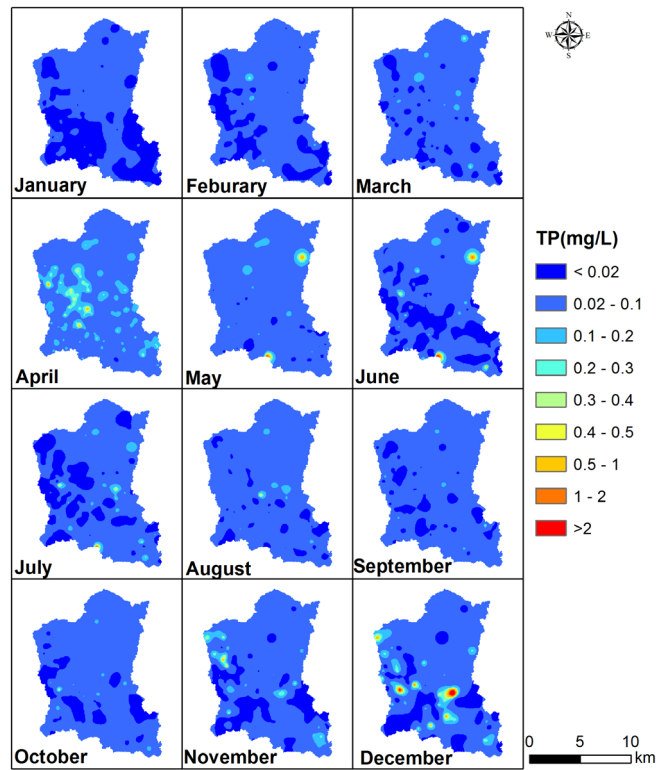


Figure 6. Estimated TP over Jinjing catchment from January to December in 2011 monthly, mg/L.

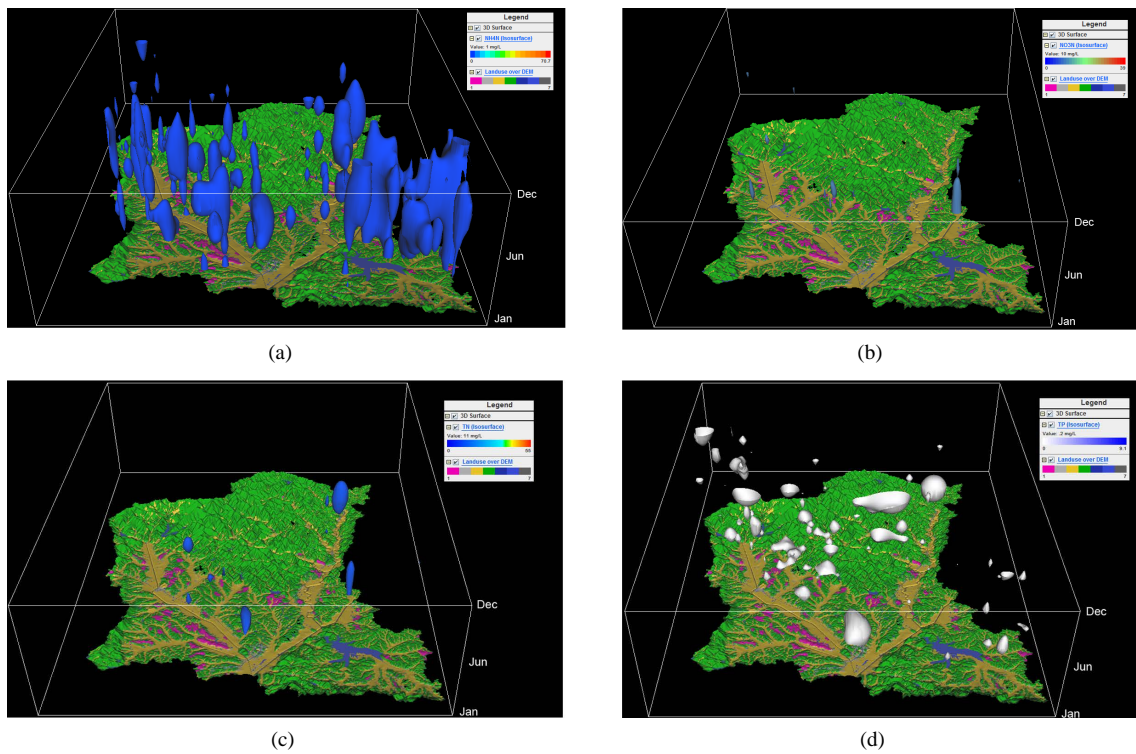


Figure 7. Three dimensional display for spatio-temporal dynamic variation of contaminated area of ammonium nitrogen (a), nitrate nitrogen (b), total nitrogen (c) and total phosphorus (d).

year 2011. According to the spatio-temporal variability of  $\text{NH}_4\text{N}$ ,  $\text{NO}_3\text{N}$ , TN and TP, the contaminated area was small, only appeared in small dispersed patches, however, close attention should be paid to the shallow ground water quality because local farmers obtain their drinking water directly from domestic wells without any treatment and potential harmful effects on human health are considerable. Moreover, closer attention should be paid to the scientific explanation and fundamental understanding of other variables governing spatial variation and temporal processes which are related to these four variables addressed in this study.

Highlighting the contaminated area over time plays a significant role for decision makers to protect public health and maintain sustainable development of the catchment. Modeling the spatio-temporal variability can improve our ability to characterize and predict the contaminated area. In this study, 3D kriging was used to investigate the spatio-temporal variability of shallow groundwater quality based on the Leave-One-Out cross-validation analysis for the year of 2011. However, limitations should be pointed out because of the small density of sampling locations in the northeast of the catchment, which is mainly dominated by woodland. As it is hilly and there are few residents in this area, there are less observational points.

## Acknowledgements

This work was financially supported by the National Basic Research Program of China (2012CB417105), the Chinese Academy of Sciences (KZCX2-YW-T07 and 100-Talents Program) and the State Administration of Foreign Experts Affairs of China (20100491005-8).

## References

- [1] Bouman, B.A.M., Castaneda, A.R. and Bhuiyan, S.I. (2002) Nitrate and Pesticide Contamination of Groundwater under Rice-Based Cropping Systems: Past and Current Evidence from the Philippines. *Agriculture, Ecosystems & Environment*, **92**, 185-199. [http://dx.doi.org/10.1016/S0167-8809\(01\)00297-3](http://dx.doi.org/10.1016/S0167-8809(01)00297-3)
- [2] Fan, A.M. and Steinberg, V.E. (1996) Health Implications of Nitrate and Nitrite in Drinking Water: An Update on Methemoglobinemia Occurrence and Reproductive and Developmental Toxicity. *Regulatory Toxicology and Pharmacology*, **23**, 35-43. <http://dx.doi.org/10.1006/rtph.1996.0006>
- [3] Holman, I.P., Howden, N.J.K., Bellamy, P., Willby, N., Whelan, M.J. and Rivas-Casado, M. (2010) An Assessment of the Risk to Surface Water Ecosystems of Groundwater P in the UK and Ireland. *Science of the Total Environment*, **408**, 1847-1857. <http://dx.doi.org/10.1016/j.scitotenv.2009.11.026>
- [4] Schot, P.P. and Pieber, S.M. (2012) Spatial and Temporal Variations in Shallow Wetland Groundwater Quality. *Journal of Hydrology*, **422**, 43-52. <http://dx.doi.org/10.1016/j.jhydrol.2011.12.023>
- [5] Mitchell, R.J., Babcock, R.S., Gelinas, S., Nanus, L. and Stasney, D.E. (2003) Nitrate Distributions and Source Identification in the Abbotsford-Sumas Aquifer, Northwestern Washington State. *Journal of Environmental Quality*, **32**, 789-800. <http://dx.doi.org/10.2134/jeq2003.7890>
- [6] Morari, F., Lugato, E., Polese, R., Berti, A. and Giardini, L. (2012) Nitrate Concentrations in Groundwater under Contrasting Agricultural Management Practices in the Low Plains of Italy. *Agriculture, Ecosystems & Environment*, **147**, 47-56. <http://dx.doi.org/10.1016/j.agee.2011.03.001>
- [7] Eckhardt, D.A.V. and Stackelberg, P.E. (1995) Relation of Ground-Water Quality to Land Use on Long Island, New York. *Ground Water*, **33**, 1019-1033. <http://dx.doi.org/10.1111/j.1745-6584.1995.tb00047.x>
- [8] Liu, G.D., Wu, W.L. and Zhang, J. (2005) Regional Differentiation of Non-point Source Pollution of Agriculture-Derived Nitrate Nitrogen in Groundwater in Northern China. *Agriculture, Ecosystems & Environment*, **107**, 211-220. <http://dx.doi.org/10.1016/j.agee.2004.11.010>
- [9] Kaown, D., Hyun, Y., Bae, G.-O. and Lee, K.-K. (2007) Factors Affecting the Spatial Pattern of Nitrate Contamination in Shallow Groundwater. *Journal of Environmental Quality*, **36**, 1479-1487. <http://dx.doi.org/10.2134/jeq2006.0361>
- [10] Puckett, L.J., Tesoriero, A.J. and Dubrovsky, N.M. (2011) Nitrogen Contamination of Surficial Aquifers—A Growing Legacy. *Environmental Science & Technology*, **45**, 839-844. <http://dx.doi.org/10.1021/es1038358>
- [11] Chen, X.M., Wo, F., Chen, C. and Fang, K. (2010) Seasonal Changes in the Concentrations of Nitrogen and Phosphorus in Farmland Drainage and Groundwater of the Taihu Lake Region of China. *Environmental Monitoring and Assessment*, **169**, 159-168. <http://dx.doi.org/10.1007/s10661-009-1159-3>
- [12] Zhang, W.L., Tian, Z.X., Zhang, N. and Li, X.Q. (1996) Nitrate Pollution of Groundwater in Northern China. *Agriculture, Ecosystems & Environment*, **59**, 223-231. [http://dx.doi.org/10.1016/0167-8809\(96\)01052-3](http://dx.doi.org/10.1016/0167-8809(96)01052-3)
- [13] Kilroy, G. and Coxon, C. (2005) Temporal Variability of Phosphorus Fractions in Irish Karst Springs. *Environmental Geology*, **47**, 421-430. <http://dx.doi.org/10.1007/s00254-004-1171-4>

- [14] Sharpley, A.N. and Rekolainen, S. (1997) Phosphorus in Agriculture and Its Environmental Implications. In: Tunney, H., Carton, O.T., Brookes, P.C. and Johnston, A.E., Eds., *Phosphorus Loss from Soil to Water. Proceedings of a Workshop*, Wexford, 29-31 September 1995, 1-53.
- [15] Sonneveld, M.P.W., de Vos, J.A., Kros, J., Knotters, M., Frumau, A., Bleeker, A. and de Vries, W. (2012) Assessment of N and P Status at the Landscape Scale Using Environmental Models and Measurements. *Environmental Pollution*, **162**, 168-175. <http://dx.doi.org/10.1016/j.envpol.2011.11.020>
- [16] Huang, H.C., Martinez, F., Mateu, J. and Montes, F. (2007) Model Comparison and Selection for Stationary Space-Time Models. *Computational Statistics & Data Analysis*, **51**, 4577-4596. <http://dx.doi.org/10.1016/j.csda.2006.07.038>
- [17] Cressie, N. and Huang, H.C. (1999) Classes of Nonseparable, Spatio-Temporal Stationary Covariance Functions. *Journal of the American Statistical Association*, **94**, 1330-1339. <http://dx.doi.org/10.1080/01621459.1999.10473885>
- [18] Gneiting, T. (2002) Nonseparable, Stationary Covariance Functions for Space-Time Data. *Journal of the American Statistical Association*, **97**, 590-600. <http://dx.doi.org/10.1198/016214502760047113>
- [19] De Cesare, L., Myers, D.E. and Posa, D. (2001) Estimating and Modeling Space-Time Correlation Structures. *Statistics & Probability Letters*, **51**, 9-14. [http://dx.doi.org/10.1016/S0167-7152\(00\)00131-0](http://dx.doi.org/10.1016/S0167-7152(00)00131-0)
- [20] De Iaco, S., Myers, D.E. and Posa, D. (2001) Space-Time Analysis Using a General Product-Sum Model. *Statistics & Probability Letters*, **52**, 21-28. [http://dx.doi.org/10.1016/S0167-7152\(00\)00200-5](http://dx.doi.org/10.1016/S0167-7152(00)00200-5)
- [21] Akita, Y., Carter, G. and Serre, M.L. (2007) Spatiotemporal Nonattainment Assessment of Surface Water Tetrachloroethylene in New Jersey. *Journal of Environmental Quality*, **36**, 508-520. <http://dx.doi.org/10.2134/jeq2005.0426>
- [22] Gräler, B., Gerharz, L. and Pebesma, E. (2011) Spatio-Temporal Analysis and Interpolation of PM10 Measurements in Europe, ETC/ACM Technical Paper 2011/10. [http://acm.eionet.europa.eu/reports/ETCACM\\_TP\\_2011\\_10\\_spatio-temp\\_AQinterpolation](http://acm.eionet.europa.eu/reports/ETCACM_TP_2011_10_spatio-temp_AQinterpolation)
- [23] Li, Y., Fu, X.Q., Liu, X.L., Shen, J.L., Luo, Q., Xiao, R.L., Li, Y.Y., Tong, C.L. and Wu, J.S. (2013) Spatial Variability and Distribution of N<sub>2</sub>O Emissions from a Tea Field during the Dry Season in Subtropical Central China. *Geoderma*, **193-194**, 1-12. <http://dx.doi.org/10.1016/j.geoderma.2012.10.008>
- [24] Deutsch, C.V. and Journel, A.G. (1998) GSLIB: Geostatistical Software Library and User's Guide. 2nd Edition, Oxford University Press, Oxford.
- [25] R Core Team (2013) R: A Language and Environment for Statistical Computing. R Foundation for Statistical Computing, Vienna. <http://www.r-project.org/>
- [26] Cambardella, C.A., Moorman, T.B., Novak, J.M., Parkin, T.B., Karlen, D.L., Turco, R.F. and Konopka, A.E. (1994) Field-Scale Variability of Soil Properties in Central Iowa Soils. *Soil Science Society of America Journal*, **58**, 1501-1511. <http://dx.doi.org/10.2136/sssaj1994.03615995005800050033x>
- [27] Addiscott, T.M. and Thomas, D. (2000) Tillage, Mineralization and Leaching: Phosphate. *Soil and Tillage Research*, **53**, 255-273. [http://dx.doi.org/10.1016/S0167-1987\(99\)00110-5](http://dx.doi.org/10.1016/S0167-1987(99)00110-5)

Scientific Research Publishing (SCIRP) is one of the largest Open Access journal publishers. It is currently publishing more than 200 open access, online, peer-reviewed journals covering a wide range of academic disciplines. SCIRP serves the worldwide academic communities and contributes to the progress and application of science with its publication.

Other selected journals from SCIRP are listed as below. Submit your manuscript to us via either [submit@scirp.org](mailto:submit@scirp.org) or **Online Submission Portal**.

